Jurnal Kejuruteraan 33(2) 2021: 293-316
https://doi.org/10.17576/jkukm-2021-33(2)-15

Computer Aided Simulation POME Biogas Purification System

Andrew Yap Kian Chung* & Ummi Kalsum Hasanah M.N
Milling and Processing Unit,
Engineering & Processing Division, Malaysian Palm Oil Board (MPOB)
No.6 Persiaran Institusi Bandar Baru Bangi,
43000 Kajang, Selangor, Malaysia.

**Corresponding author: andrew@mpob.gov.my*

Received 19 January 2020, Received in revised form 12 May 2020
Accepted 21 September 2020, Available online 30 May 2021

ABSTRACT

About three (3) tonnes of palm oil mill effluent (POME) is generated when one (1) tonne of crude palm oil (CPO) is produced. Microbial digestion treatment is commonly used in Malaysian palm oil mills due to the low capital expenditure (CAPEX) and operational expenditure (OPEX). However, anaerobic digestion of POME produces methane gas which is 21 times more harmful than carbon dioxide. 1m^3 of POME could generate 27m^{3}of biogas at standard temperature and pressure with approximate caloric value of 20 MJm^{-3} under optimum conditions Thus, methane capturing biogas plant to address sustainability issue is included as part of effluent treatment plant. Many mills start to utilise the biogas energy to replace palm kernel shell which could be sold as renewable solid fuel. Although untreated biogas may be good enough for boiler fuel, internal combustion engines need a fairly homogeneous fuel with methane (CH_4) content up to 80 % and hydrogen sulphite (H_2S) content less than 200 ppm in order to ensure the optimum engine performance. Water scrubber system is widely used in gas purification. Computer aided biogas purification system simulation involving water scrubber and flashing drum is presented in the effort to produce IC engine fuel. ChemCAD simulation result shows that POME biogas purification process is feasible at 10 bar pressure and 25°C ambient temperature.

Keyword: Biogas; carbon dioxide; ChemCAD; palm oil mill effluent; water scrubber

INTRODUCTION

Malaysia produced 19,858,367 tonnes of crude palm oil in year 2019 (MPOB 2020). About three (3) tonnes of palm oil mill effluent (POME) with average characteristic as shown in Table 1 is generated when one (1) tonne of crude palm oil (CPO) is produced.

POME is non-toxic but pollutes aquatic environments due to its high biological oxygen demand. Department of Environment enforces regulatory standards that require mill operators to treat POME before discharging it into waterways. Because of low capital expenditure and operational simplicity, almost all palm oil mills practise open ponding treatment systems. However, anaerobic organic decomposition as shown in Figure 1 releases into the atmosphere methane gas, which is a greenhouse gas (GHG) 21 times more harmful than carbon dioxide (EPA 2011). Thus sustainability issue need to be addressed (Loh et al. 2017).

Anaerobic digestion of POME produces biogas which is a mixture of gases as shown in Table 2. At standard temperature and pressure, 1 m^3 of POME could generate 27 m^3 biogas with approximate caloric value of 20 MJm^{-3} under optimum conditions as shown in Table 3. The actual biogas calorific value is a function of CH_4 percentage, temperature and absolute pressure (Stefan, 2004). Thus, biogas capture is a feasible solution whereby renewable energy is generated while reducing environmental GHG impact.

Several technologies for effluent anaerobic digestion are readily available. Ample contact between microorganisms and substrate is essential in all designs beside microorganisms wash out prevention. Due to high solids and oil content in POME, either continuous stir tank reactors (CSTR) or covered lagoons is preferred for palm oil mills. General biogas plant process flow chart is shown in Figure 2.

PROBLEM STATEMENT

Untreated biogas may be good enough for boiler fuel but not for internal combustion gas engine in electricity generation with efficiency between 36% and 42%. Thus, biogas needs to be treated to reduce impurities and becomes a fairly homogeneous fuel with methane (CH_4) content up to 80 % and hydrogen sulphite (H_2S) content of less than 200 ppm.

TABLE 1. Average raw POME characteristic

Symbol	Parameters	Unit	Average
BOD	Biological Oxygen Demand	mgl^{-1}	25000
COD	Chemical Oxygen Demand	mgl^{-1}	50000
TSS	Total Suspended Solid	mgl^{-1}	31170
AN	Ammonia (NH_3-N)	mgl^{-1}	41
O&F	Oil and Fat	mgl^{-1}	3075
pH	pH		4

Source: Ahmad Parveez et al. (2020).

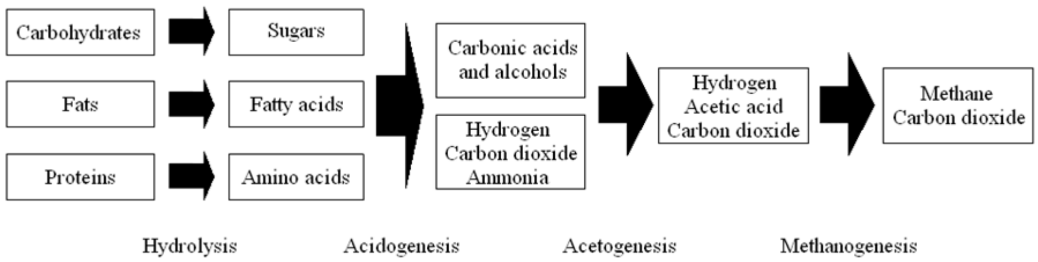

FIGURE 1. Anaerobic digestion stages

TABLE 2. Biogas compositions

Elements	Formula	Concentration (Vol. %)
Methane	CH_4	50–75
Carbon dioxide	CO_2	25–45
Water vapour	H_2O	2–7
Oxygen	O_2	< 2
Nitrogen	N_2	< 2
Hydrogen Sulphite	H_2S	< 2
Ammonia	NH_3	< 1
Hydrogen	H_2	< 1

OBJECTIVE

The objective of this paper is to simulate biogas purification system involving water scrubber and flashing drum for scrubbing water recovery.

WATER SCRUBBER

Water scrubber is a counter current packed column as shown in Figure 3 where gas-liquid extraction reduces CO_2 concentration to enrich the methane content to above 80% and H_2S concentration typically below 200 ppm in order to avoid excessive corrosion in the internal combustion engine (Gautam 2014).

Packing materials are designed to maximize the liquid surface area per unit bed volume to enhance mass transfer coefficient. Void fraction, ε, is a crucial parameter to characterize two-phase flows as occur in the biogas packed column water scrubber. Various geometric definitions as shown in Equation (1) are used to define the void fraction where $f(r,t)$ is local instantaneous at radius r and time t, L_G is beam line length through vapor phase, L_L is beam line length through liquid phase, A_G is vapor phase channel cross-section area, A_L is liquid phase channel cross-section area, V_G is vapor phase channel volume and V_L is liquid phase channel volume (Thome 2004).

$$
\begin{aligned}
&\text{Local} && \varepsilon(r,t) = \frac{1}{t}\int_t f(r,t)\,dt \\
&\text{Chordal} && \varepsilon = \frac{L_G}{L_G + L_L} \\
&\text{Cross-sectional} && \varepsilon = \frac{A_G}{A_G + A_L} \\
&\text{Volumetric} && \varepsilon = \frac{V_G}{V_G + V_L}
\end{aligned}
\qquad (1)
$$

TABLE 3. Optimum biogas formation conditions

Parameter	Units	Range	Remark
Temperature	°C	35 – 38 55 – 57	Mesophilic microbe Thermophilic microbe
Hydraulic Retention Time	day	20 – 50	Effluent dependent
COD Concentration	mgl^{-1}	< 80,000	Effluent dependent
Ratio POME:FFB	m^3 $tonne^{-1}$	0.6 – 1	Mill process dependent
pH Value		6.7–7.5	During anaerobic digestion

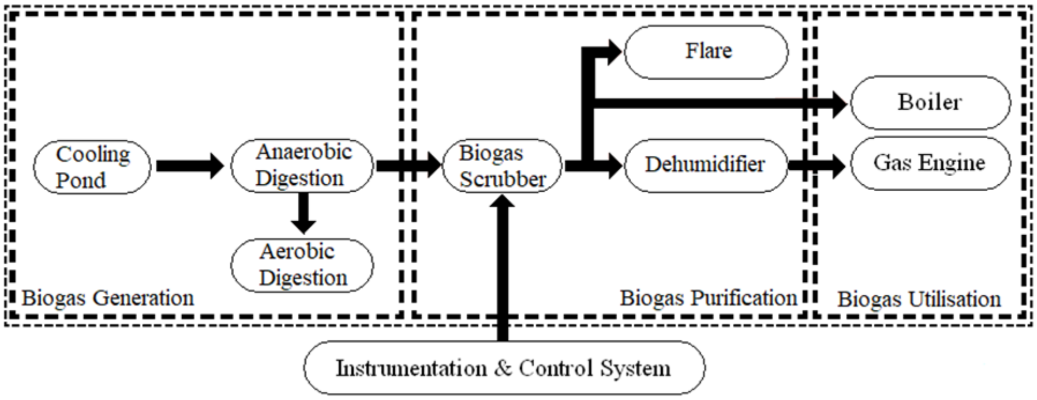

FIGURE 2. General biogas plant process flow chart

Pressure drop, $-\Delta P$, due to friction when fluid flows through a packed bed is shown in Equation (2) known as Darcy (1896) relationship where H is the packed bed height [m] and U is superficial fluid velocity [m/s].

$$\frac{-\Delta P}{H} \propto U \tag{2}$$

Empiric data regression for non-spherical particles random packed bed known as Ergun equation is shown in Equation (3) where μ is dynamic viscosity, ε is packing void fraction, x_e is packing equivalent spherical diameter and ρ is fluid density.

$$\frac{-\Delta P}{H} = 150\frac{\mu U(1-\varepsilon)^2}{x_e^2\varepsilon^3} + 1.75\frac{\rho U^2(1-\varepsilon)}{x_e\varepsilon^3} \tag{3}$$

Assuming biogas is a multi-components ideal gas mixture, if the biogas solute component forms a simple solution with small concentration in liquid phase, solubility could be determined by Henry's equation as shown in Equation (4) where C_s is gas equilibrium solubility in a particular solvent at a fixed temperature, k is Henry's law constant and P_G is the respective G gas partial pressure (Ralph & Strigle, 1994).

$$P_G = kC_s \tag{4}$$

The biogas water scrubber is designed based on the CO_2 content in the raw biogas which will be absorbed and dissolves in water to form carbonic acid (H_2CO_3).

$$CO_2 + H_2O \rightleftarrows H_2CO_3$$

Henry's constant (k) for CO_2 in H_2O at atmospheric pressure and temperature 298K is 1.67×10^8 Pa and correlation for pressures below 1 MPa is shown as Equation (5) where T is temperature in Kelvin (Carroll et al. 1991).

More CO_2 solubility data is given in Appendix and presented in Figure 4. However, the water absorption process also removes H_2S at low concentration (Nock et al. 2014). Practical data from an operating plant in Malaysia shows that H_2S content in raw POME biogas was reduced from 3500 ppm to 50 ppm in average using water scrubber at atmospheric pressure and ambient temperature.

Absorption operation in packed column is related to two-film mass transfer theory for a solute from the gas phase to liquid phase which is governed essentially by molecular diffusion. The mass transfer coefficient is defined as diffusivity related to mass transfer rate, mass transfer area and concentration change as driving force. The overall gas-phase mass transfer coefficient, K_G for an unknown system can be approximated based on an available known system as shown in

$$\ln(k^{-1}) = -6.8346 + 1.2817\times10^4T^{-1} - 3.7668\times10^6T^{-2} + 2.997\times10^8T^{-3}$$
$$273\text{ K} < T < 433\text{ K} \tag{5}$$

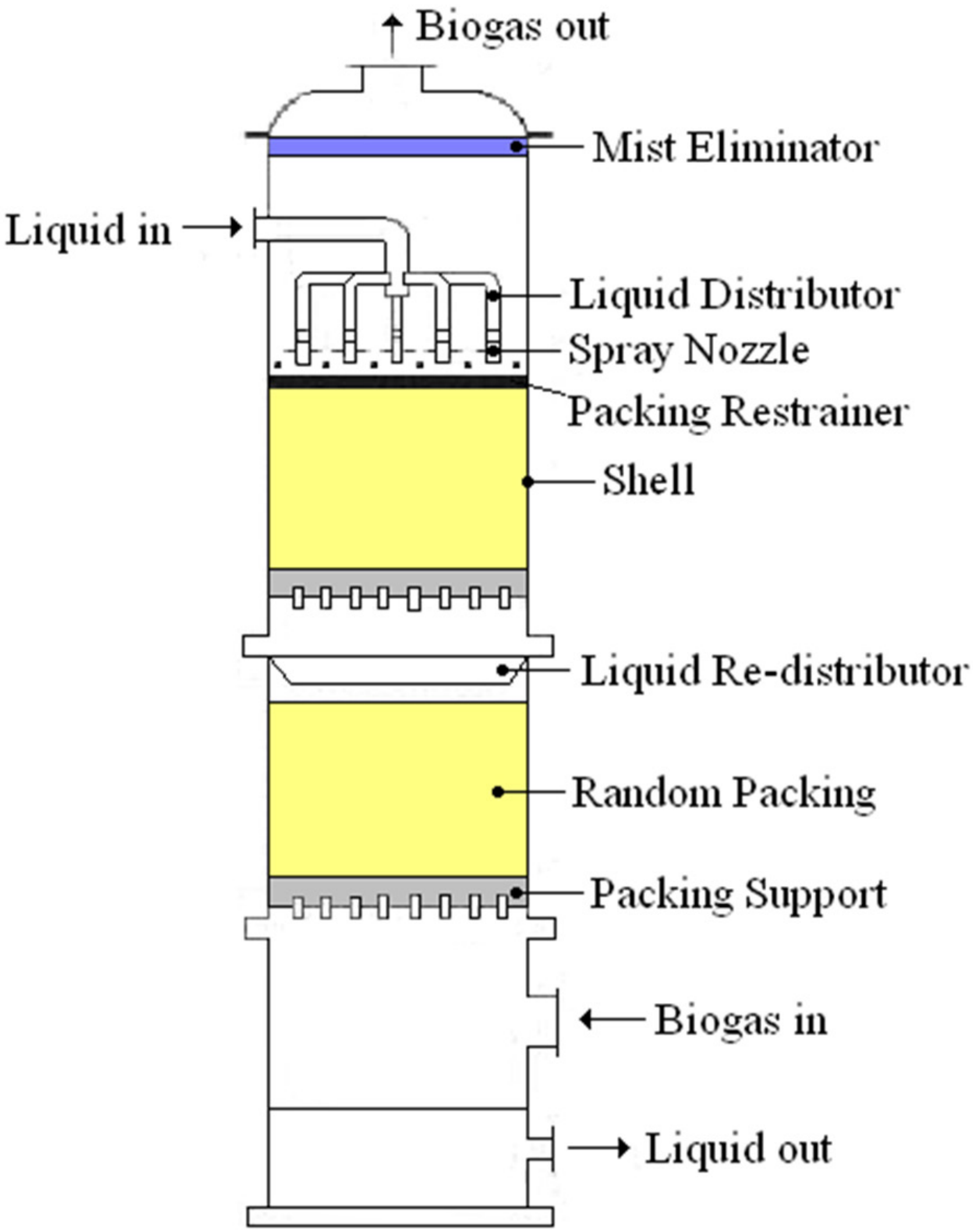

FIGURE 3. Biogas water scrubber

$$(K_G\alpha)_{unknown} = (K_G\alpha)_{known}\left(\frac{D_v^{unknown}}{D_v^{known}}\right)^{0.36}\left[\text{lb mol}\left(\text{h ft}^3\text{atm}\right)^{-1}\right] \quad (6)$$

Equation (6) where α is interfacial area and D_v is solute diffusivity in gas [ft^2h^{-1}] (Branan 2002).

If the heat of solution in the liquid phase is negligible and gas stream solute concentration is low, the required tower packing volume, V_p is determined using Equation (7) where ΔP is partial pressure driving force at inlet ($_1$) and outlet ($_2$).

$$V_p = \frac{F_B(P_{C1} - P_{C2})}{P_T K_G \alpha \Psi}; \Psi = \frac{\Delta P_1 - \Delta P_2}{\ln(\frac{\Delta P_1}{\Delta P_2})} \quad (7)$$

If the operating line is straight and the solvent feed is solute free in straight equilibrium curve with slope *m*, the transfer unit number, N_T is defined as Equation (8) where *y* is mole fraction in vapor phase and is plotted in Figure 5 for $0 \leq \beta \leq 0.9$.

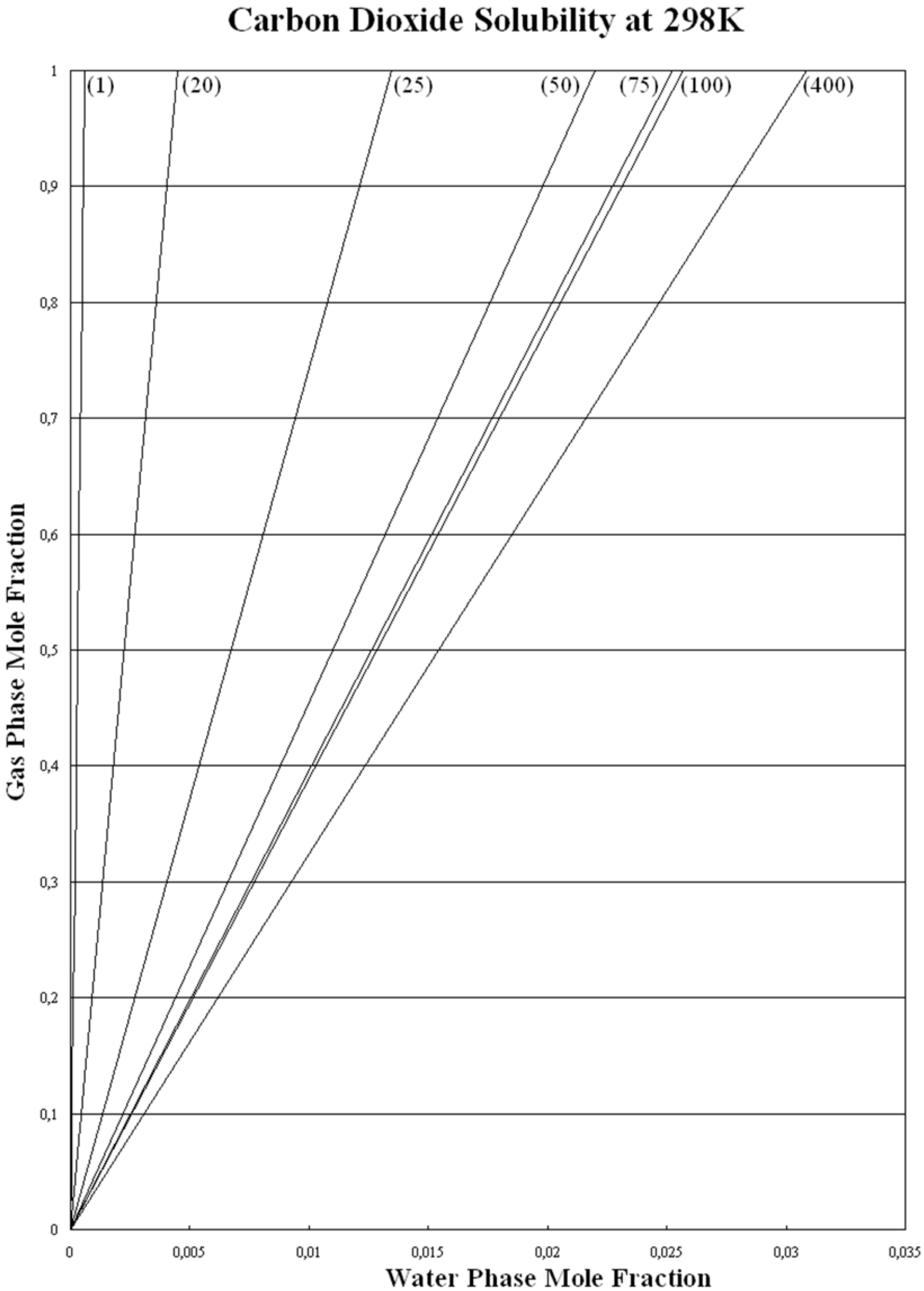

Number in bracket () indicates the Total Pressure in [atm]

FIGURE 4. CO_2 solubility equilibrium for various pressures at 25°C

$$N_T = \frac{1}{(1-\beta)} \ln[(1-\beta)\frac{y_1}{y_2} + \beta] \text{ where } \beta = m\frac{F_B}{F_L} \quad (8)$$

The column cross sectional area, A is a function of superficial fluid velocity (U) which is defined in the Generalized Pressure Drop Correlation for a selected pressure drop based on flow parameter,

$$F_{LV} = \frac{F_L}{F_B}\sqrt{\frac{\rho_v}{\rho_L}}$$

where F_L is liquid flow rate [kgs^{-1}], ρ_v is gas density [kgm^{-3}] and ρ_L is liquid density [kgm^{-3}]. Determination of column cross sectional area required and column diameter are shown in Equation (9).

$$A = \frac{F_B}{U}\left[m^2\right]; D = \sqrt{\frac{4A}{\pi}}\left[m\right]; \pi = \frac{22}{7} \quad (9)$$

Onda *et. al.* (1968) defined empiric correlations for film mass transfer coefficients and effective wetted packing area, A_w to determine film transfer unit heights as shown in Equation (10) to Equation (13).

Pressure drop for random packed column should be less than 80mm H_2O per meter packing. Packing size selection, x_e is usually based on column diameter, D. For D < 0.3m, then x_e < 25mm. If 0.3m ≤ D ≤ 0.9m, x_e would be in the range of 25mm to 38mm and for D > 0.9m, range of x_e would be 50mm to 75mm. Large packing size in small column may cause poor liquid distribution (Coulson et al. 1989).

SIMULATION

A 60-tonne mill with ten (10) hours daily operation will generate about 360m^3 of POME per day which in turn produces about 9720 m^3 of biogas during steady state at standard temperature and pressure (STP). If the biogas plant operated for 24 hours per day, the biogas scrubber needs to treat 0.1125 m^{3}s^{-1} of biogas. The basic design parameter is shown in Table 4. It is required to remove 95% CO_2. The operation unit schematic is shown in Figure 6.

From the CO_2 solubility data given in Appendix, Table A1, higher solubility is achieved with higher pressure and lower temperature. However, high pressure equipment incurs higher CAPEX and high process temperature manipulation requires higher OPEX. Thus, based on Figure 4, the biogas water scrubber that operates at 25°C and 10 atm would be appropriate. The washed water could be recovered by flashing off solute carbon dioxide from pressure 10 atm to 1 atm which will require much lower OPEX compared to heat recovery.

Partial pressure of CO_2 in the feed,

$$P_{C1} = 0.35 \text{ X } 1000 = 350 \text{ kPa}$$

Partial pressure of CO_2 in the exit,

$$P_{C2} = 350 \text{ X } 0.05 = 17.5 \text{ kPa (95\% recovery)}$$

$$\text{Thus} \frac{y_1}{y_2} = \frac{P_{C1}}{P_{C2}} = \frac{350}{17.5} = 20.$$

The equilibrium slope, *m* at pressure 10 atm is

$$m = \frac{y}{x} = \frac{1}{C_s} = \frac{k}{P_G} = \frac{1.67\times10^8}{10\times100000} = 167$$

Since the equilibrium slope is steep, maximum number of stages may be needed. From Figure 5 for $\frac{y_1}{y_2} = 20$, maximum N_T = 18 at $m\frac{F_B}{F_L} \dashrightarrow 1.0$.

Material balance for the water scrubber operation unit above yield

$$F_L x_1 = F_B(0.35 \times 0.95)$$

$$x_1 = \frac{F_B}{F_L}(0.3325) = \frac{mF_B}{mF_L}(0.3325)$$

$$x_1 = \frac{m}{167}\frac{F_B}{F_L}(0.3325) = \frac{0.3325}{167}$$

x_1 = 1.9910 × 10^{-3} mol fraction of CO_2 in water phase.

COLUMN DIAMETER DETERMINATION

Assuming that biogas is an ideal gas; the molar volume of an ideal gas at pressure 100 kPa and temperature 0°C (STP) is (Winterbone & Turan, 2015)

$$\frac{A_w}{\alpha} = 1 - exp[-1.45(\frac{\sigma_c}{\sigma_L})^{0.75}(\frac{F_L^*}{\alpha\mu_L})^{0.1}(\frac{F_L^{*2}\alpha}{g\rho_L^2})^{-0.05}(\frac{F_L^{*2}}{\rho_L\sigma_L\alpha})^{0.2} \quad (10)$$

$$k_L\left(\frac{\rho_L}{g\mu_L}\right)^{1/3} = 0.0051\left(\frac{F_L^*}{A_w\mu_L}\right)^{2/3}\left(\frac{\mu_L}{\rho_L D_L}\right)^{-1/2}(\alpha x_e)^{0.4} \quad (11)$$

$$\frac{k_G RT}{\alpha D_v} = K\left(\frac{F_B^*}{\alpha\mu_v}\right)^{0.7}\left(\frac{\mu_v}{\rho_v D_v}\right)^{1/3}(\alpha x_e)^{-2}; \quad (12)$$
$$K = 5.23 \text{ if } x_e > 15\text{mm}; K = 2.00 \text{ if } x_e \le 15\text{mm}$$

$$H_G = \frac{F_B}{k_G A_w P_T}; H_L = \frac{F_L}{k_L A_w(\frac{\rho_L}{W_{H2O}})} \quad (13)$$

$$\frac{RT}{P} = \frac{8314.5\times273.15}{100000} = 22.7111 \text{ m}^3\text{kmol}^{-1}$$
$$= 0.0227 \text{ m}^3\text{mol}^{-1}$$

Molecular weight for biogas is

$$[(16\times0.65) + (44\times0.35)] = 10.4 + 15.4 = 25.8$$

Biogas flow rate,

TABLE 4. Basic design parameters

Particular	Symbol	Value
Biogas inlet pressure	P_T	1000 kNm^{-2}
Inlet temperature	T_i	25°C (298 K)
Carbon dioxide content in raw biogas	C	35% v/v
Molecular weight carbon dioxide (CO_2)	W_{CO2}	44
Molecular weight water (H_2O)	W_{H2O}	18
Molecular weight methane (CH_4)	W_{CH4}	16
Water density at 25°C	ρ_L	997.13 kgm^{-3}
Water molar density	λ	55600 mol m^{-3}
Water viscosity at 25°C	μ_L	0.0008891 Nsm^{-2}
Water surface tension at 25°C	σ	0.07187 Nm^{-1}
Carbon dioxide density at 25°C, 10bar	ρ_v	18.725 kgm^{-3}
Carbon dioxide viscosity at 25°C, 10bar	μ_v	15.02×10^{-6} Nsm^{-2}
Universal gas constant	R	8314.5 $J(kmol.K)^{-1}$
Gravitational acceleration	g	9.81 ms^{-2}
Critical Surface Tension for Particular Packing Material		
Ceramic = 61 mNm^{-1} Metal = 75 mNm^{-1}	Plastic = 33 mNm^{-1}	Carbon = 56 mNm^{-1}

(Source: Coulson et al. 1989)

$$F_B = \frac{0.1125}{0.0227} = 4.9559 \text{ mol s}^{-1} = 0.1279 \text{ kgs}^{-1}$$

Water flow rate,

$$F_L = \frac{m}{1.0} F_B = \frac{167}{1.0} \times 4.9559 = 827.6353 \text{ mol s}^{-1}$$
$$F_L = 14.8974 \text{ kgs}^{-1}$$

Biogas density at 10 atm, 25°C,

$$\rho_V = \frac{25.8P}{RT} = \frac{25.8\times1000000}{8314.5\times298.15} = 10.4076 \text{ kgm}^{-3}$$

Water kinematic viscosity at 25°C,

$$\frac{\mu_L}{\rho_L} = \frac{0.0008891}{997.13} = 8.9166\times10^{-7}\, m^2 s^{-1}$$

$$F_{LV} = \frac{F_L}{F_B}\sqrt{\frac{\rho_V}{\rho_L}} = \frac{14.8974}{0.1279}\sqrt{\frac{10.4076}{997.13}} = 11.9$$

From Figure 7, design for a pressure drop of 4mm H_2O/m packing, extended graph shows that

$$\frac{42.9 F_p U^2 (\frac{\mu_L}{\rho_L})^{0.1}}{\rho_V(\rho_L - \rho_V)} = 0.008$$

where F_p is packing factor. Select 38mm Raschig rings, x_e = 38mm from Appendix Table A4, F_p = 83.

$$\frac{\left(42.9\times83\times U^2\times(8.9166\times10^{-7})^{0.1}\right)}{10.4076\times(997.13-10.4076)} = 0.008$$
$$0.0861U^2 = 0.008; U^2 = 0.0929;$$
$$U = 0.304817678 \text{ kgm}^{-2}\text{s}^{-1}$$

Column area required,

$$A = \frac{0.1279}{0.3048} = 0.4196 \text{ m}^2;$$

$$\text{Diameter, } D = \sqrt{\frac{4\times0.4196}{\pi}} = 0.7308 \text{ m}$$

$$F_L^* = \frac{14.8974}{0.4196} = 35.5042 \text{ kgs}^{-1}\text{m}^{-2};$$

$$F_B^* = \frac{0.1279}{0.4196} = 0.3048 \text{ kgs}^{-1}\text{m}^{-2}$$

OVERALL LIQUID PHASE TRANSFER UNIT HEIGHT ESTIMATION USING ONDA'S METHOD

From Appendix Table A4, for 38 mm Metal Raschig rings, α = 130 m^2m^{-3} and σ_c = 0.075 Nm^{-1}. Based on Equation (10),

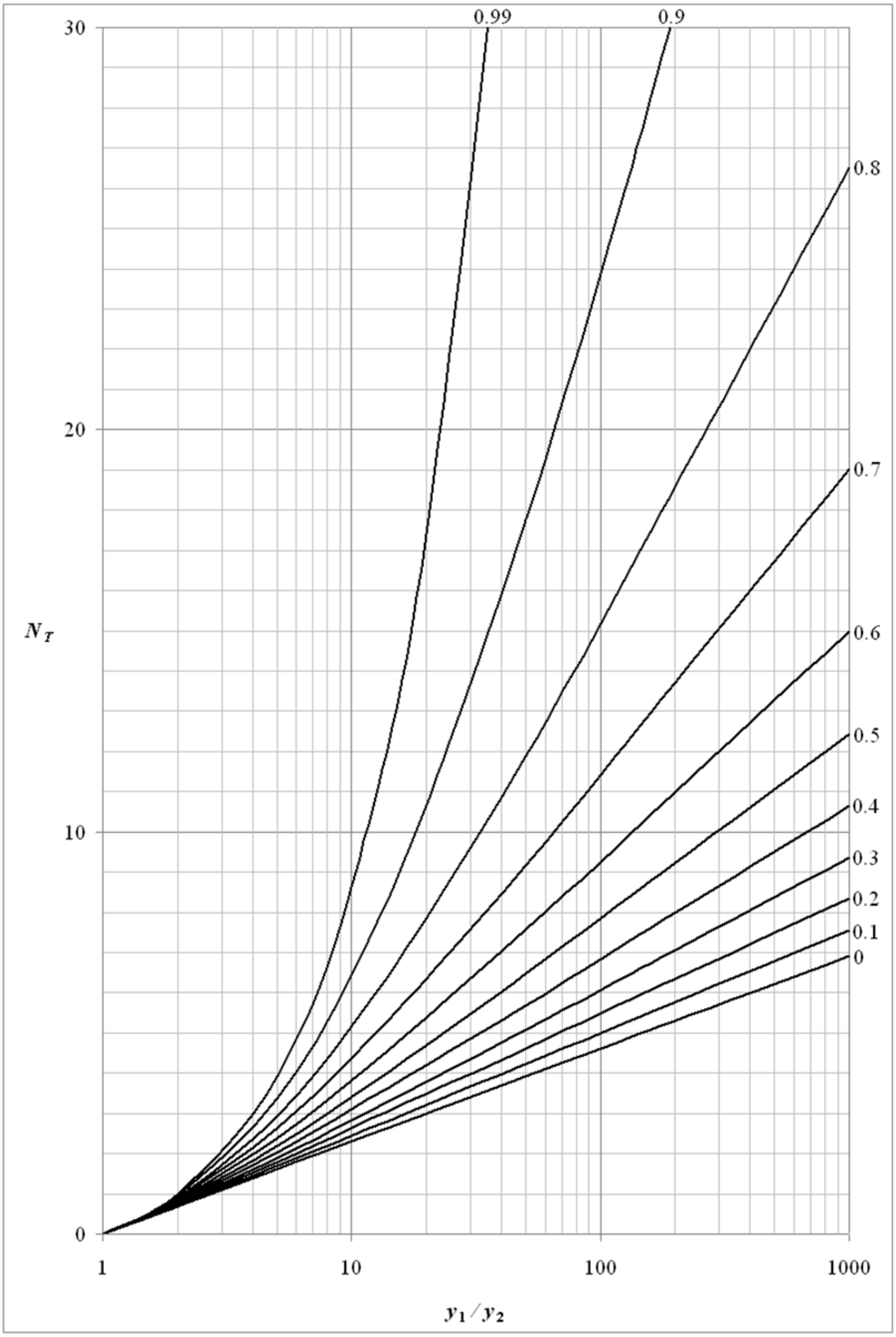

FIGURE 5. Transfer unit estimation based on mol fraction for various β values

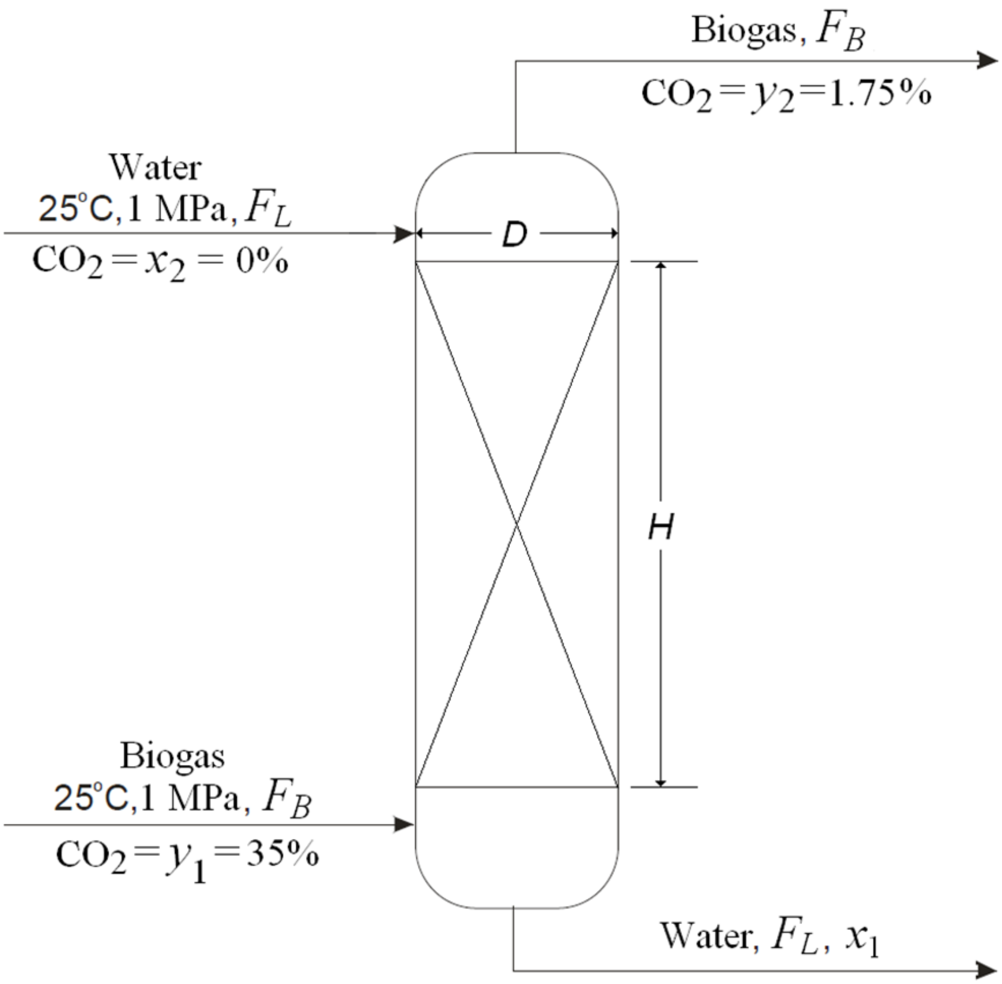

FIGURE 6. Biogas water scrubber operation unit schematic diagram

$$\left(\frac{\sigma_c}{\sigma_L}\right)^{0.75} = \left(\frac{0.075}{0.07187}\right)^{0.75} = 1.032488478$$

$$\left(\frac{F_L^*}{\alpha\mu_L}\right)^{0.1} = \left(\frac{35.5038}{0.1156}\right)^{0.1} = 1.773093756$$

$$\left(\frac{F_L^{*2}\alpha}{g\rho_L^2}\right)^{-0.05} = \left(\frac{163867.574}{9753771.404}\right)^{-0.05} = 1.226687606$$

$$\left(\frac{F_L^{*2}}{\rho_L\sigma_L\alpha}\right)^{0.2} = \left(\frac{1260.5198}{9316.2853}\right)^{0.2} = 0.6702878982$$

$$\frac{A_w}{\alpha} = 1 - e^{[-2.182630764]} = 1 - 0.11274 = 0.88726$$

$A_w = 130\times0.88726 = 115.3438\ m^2m^{-3}$

$\alpha x_e = 130\times38\times10^{-3} = 4.94$

Liquid diffusivity and gas diffusivity are determined by Wilke & Chang (1955) equation and Fuller et al. (1966) equation with data presented in Appendix, Table A5 and Table A6.

Liquid diffusivity,

$$D_L = \frac{1.173\times10^{-13}(2.6\times18)^{0.5}\times298}{0.8891\times(0.0340)^{0.6}}$$

$D_L = 3.0168\times10^{-9}\ m^2s^{-1}$

From Table A5, $v_a = (2\times1.98) + 5.48 = 9.44$

Gas diffusivity,

$$D_v = \frac{1.013\times10^{-7}\times298^{1.75}\left(\frac{1}{18}+\frac{1}{44}\right)^{0.5}}{10\times[(9.44)^{1/3}+(26.9)^{1/3}]^2}$$

$D_v = 2.679\times10^{-5}\ m^2s^{-1}$

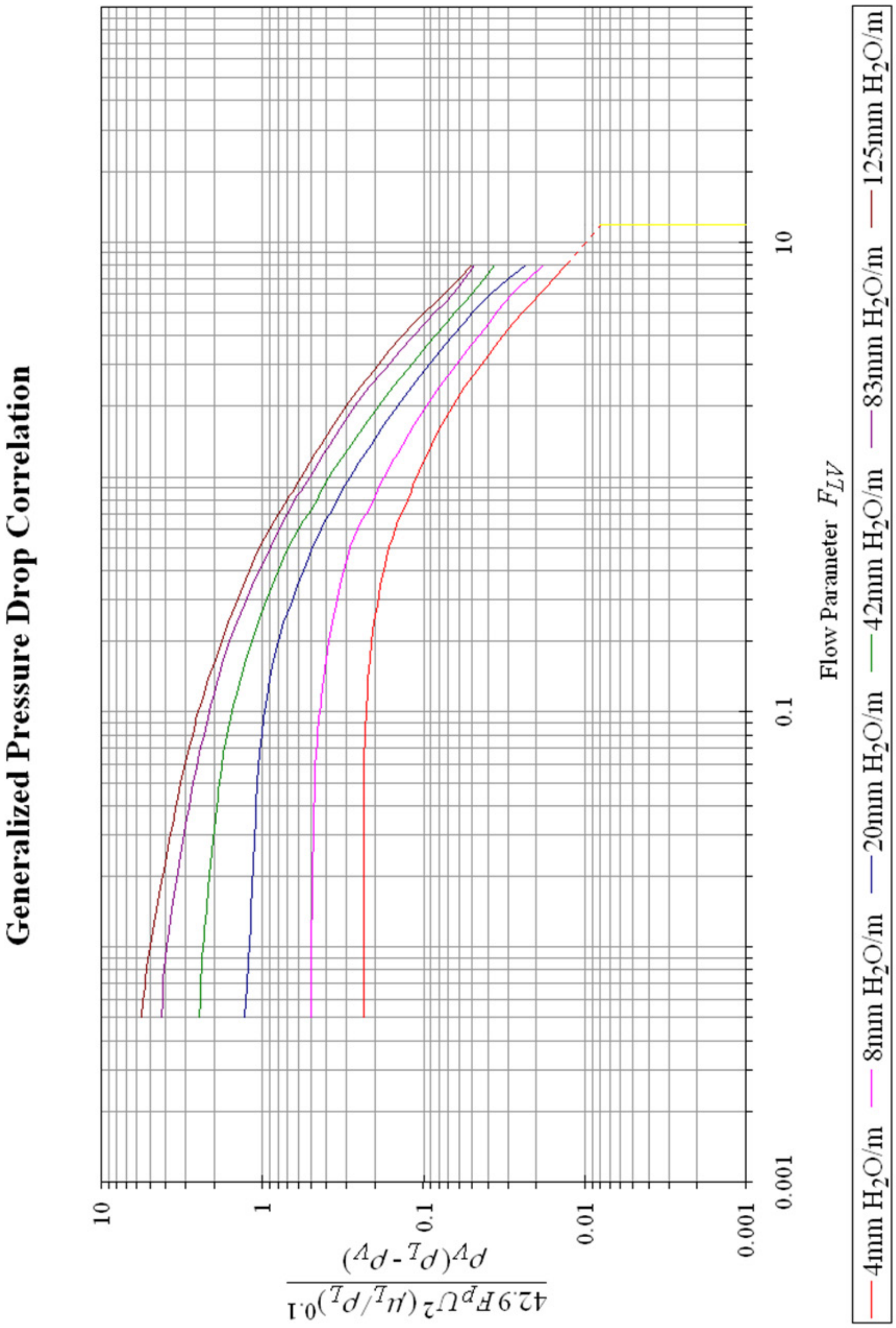

FIGURE 7. Generalized pressure drop correlation adopted from norton chemical process products corporation

$$k_L\left(\frac{997.13}{9.81\times 0.0008891}\right)^{1/3} = 48.5338k_L$$

$$\left(\frac{35.5042}{115.3438\times 0.0008891}\right)^{2/3} = 49.30488051066619$$

$$\left(\frac{0.0008891}{997.13\times 3.0168\times 10^{-9}}\right)^{-1/2} = 0.0581666223874$$

$$0.0051\times 49.3049\times 0.0582\times 1.8945 = 0.0277$$

$$48.5338k_L = 0.0277; k_L = \frac{0.0277}{48.5338} = 0.0005709 \text{ ms}^{-1}$$

$$\frac{k_G \times 0.083145 \times 298}{130 \times 2.6799 \times 10^{-5}} = 7{,}111.9789199941444k_G$$

$$\left(\frac{0.3048}{130 \times 15.02 \times 10^{-6}}\right)^{0.7} = 34.306876125174156$$

$$\left(\frac{15.02 \times 10^{-6}}{18.725 \times 2.6799 \times 10^{-5}}\right)^{1/3} = 0.31048682228401$$

$$5.23 \times 34.3069 \times 0.3105 \times 0.0410 = 2.2828224660140$$

$$7{,}111.9789199941444k_G = 2.2828224660140;$$

$$k_G = 0.000321 \text{ kmol (sm}^2\text{ bar)}^{-1}$$

$$\text{Molar flow rate } F_B = \frac{0.3048}{25.8} = 0.0118 \text{ kmol } (\text{s})^{-1};$$

$$\text{Molar flow rate } F_L = \frac{35.5042}{18} = 1.9725 \text{ kmol } (\text{s})^{-1}$$

Gas film transfer unit height,

$$H_G = \frac{0.0118}{0.000321 \times 115.3438 \times 10} = 0.0319 \text{ m}$$

Liquid film transfer unit height,

$$H_L = \frac{1.9725}{0.0005709 \times 115.3438 \times (\frac{997.13}{18})}$$

$$H_L = 0.5407 \text{ m}$$

Overall transfer unit height,

$$H_{LG} = 0.5407 + 0.0319 = 0.5726 \text{ m}$$

Pack bed height,

$$H = 0.5726 \times 18 = 10.3069 \text{ m; round to } 10.50 \text{ m}$$

From the CheCalc version 7.1.2 computer aided packed column design based on Strigle modified Eckert's Generalized Pressure Drop Correlation (GPDC) Diagram, the column flooding is 43.87%. Table 5 summarized the conceptual design result.

Based on the conceptual design result, POME biogas purification process has been successfully simulated using ChemCAD version 7.1.2 computer aided design software. Nonrandom two liquid (NRTL) thermodynamic model has been selected for global K value modeling whereas Peng-Robinson state equation has been used for vapor fugacity correction in the simulation. Practical data shows that average raw POME biogas contains 64.65% CH_4, 35% CO_2 and 0.35% H_2S. Figure 8 shows the simulated process flow diagram at 10 bars, 25°C and the respective stream properties are shown in Table 6.

Calculation mode: Simultaneous modular
Flash algorithm: Normal
Equipment Calculation Sequence: 1, 2, 5, 7, 8, 3, 6, 4
Equipment Recycle Sequence: 2, 5, 7, 8, 3, 6, 4
Recycle Cut Streams: 7
Maximum loop iterations: 40
Recycle Convergence Tolerance

- Flow rate: 1.000×10^{-3} kg/h
- Temperature: 1.000×10^{-3} °C
- Pressure: 1.000×10^{-3} bar
- Enthalpy: 1.000×10^{-3} MJ/h
- Vapour fraction: 1.000×10^{-3}

Recycle calculation has converged. Table 7 shows the process simulation mass and energy balance.

DISCUSSION

Packed columns are widely used for distillation, absorption and liquid-liquid extraction. The fluid contact in a packed column is continuous, flowing over the packing surface counter currently or co-currently. The packed column performance depends mainly on the proper fluid distribution throughout the packed bed. The principal packing requirements are to provide a large surface area for fluid interface with low flow resistance and to promote uniform fluid distribution flowing across the column cross-section. Random packing is commonly used in the process industries (Coulson et al. 1989).

Biogas gas water scrubbing is a high liquid-gas ratio process due to low solubility of CO_2 in water. The flow parameter is found to be more than 10 whereas available generalized pressure drop correlation chart is having flow parameter of less than 10. However, experimental results show that graphical correlations for various constant pressure drops is valid to be extrapolated for flow parameter range between 10 to 70 (Jaole et al. 1995).

Table 2 shows that POME biogas contain small amount of hydrogen sulfide (H_2S) but substantial amount of carbon dioxide (CO_2) which has to be removed in order for the biogas produced to be suitable for internal combustion engines fuel. Water scrubbers absorb the undesirable gases in raw biogas physically and dissolve in water. The water scrubber performance is solely depended on the solubility of the particular gas in water. Generally gas solubility increases at lower temperature but higher pressure. Due to the low solubility of CO_2 in water, biogas water scrubbing needs to be carried out at higher pressure to reduce the liquid-gas ratio in order to avoid flooding.

TABLE 5. Conceptual design result summaries for water scrubber packed column

Column diameter, D	= 0.7308 m	Biogas flow rate, F_B	= 0.1279 kgs^{-1}
Pack bed height, H	= 10.50 m	Water flow rate, F_L	= 14.8974 kgs^{-1}
Column flooding	= 43.87%	CO_2 mol frac. in water, x_1	= 1.9910×10^{-3}
Column pressure, P	= 10 bar	Column temperature	= 298 K (25°C)
Pressure drop	= 4mm H_2O /m	Metal Raschig ring 38mm	random packing

TABLE 6. Stream properties

Stream No.	1	2	3	4
Name	Raw Biogas	Compressed		Water
		Overall		
Molar flow kmol/h	22.2638	22.2638	22.2638	24.3881
Mass flow kg/h	460.4400	460.4400	460.4400	439.3522
Temperature °C	25.0000	281.1050	30.0000	25.0000
Pressure bar	1.0000	10.0000	10.0000	1.0000
Vapour mole fraction	1.000	1.000	1.000	0.0000
Enthalpy MJ/h	-2828.5	-2602.6	-2839.8	-6967.6
T_c °C	-64.4918	-64.4918	-64.4918	374.1999
P_c bar	49.1535	49.1535	49.1535	221.1821
Std. sp gr. wtr = 1	0.387	0.387	0.387	1.000
Std. sp gr. air = 1	0.714	0.714	0.714	0.622
Degree API	233.9444	233.9444	233.9444	10.0000
Average mol weight	20.6811	20.6811	20.6811	18.0150
Actual density kg/m^3	0.8365	4.4916	8.4090	996.7084
Actual volume m^3/h	550.4108	102.5122	54.7556	0.4408
Std liquid m^3/h	1.1892	1.1892	1.1892	0.4394
Std vapour 0°C m^3/h	499.0139	499.0139	499.0139	546.6268
		Vapour only		
Molar flow kmol/h	22.2638	22.2638	22.2638	
Mass flow kg/h	460.4400	460.4400	460.4400	
Average mol weight	20.6811	20.6811	20.6811	
Actual density kg/m^3	0.8365	4.4916	8.4090	
Actual volume m^3/h	550.4108	102.5122	54.7556	
Std liquid m^3/h	1.1892	1.1892	1.1892	
Std vapour 0°C m^3/h	499.0139	499.0139	499.0139	
C_p kJ/kg-K	1.7377	2.3793	1.7474	
Z factor	0.9974	0.9993	0.9759	
Viscosity N-s/m^2	1.225×10^{-5}	2.027×10^{-5}	1.260×10^{-5}	
Thermal cond W/mK	0.0303	0.0699	0.0318	
		Liquid only		
Molar flow kmol/h				24.3881
Mass flow kg/h				439.3522
Average mol weight				18.0150
Actual density kg/m^3				996.7084
Actual volume m^3/h				0.4408
Std liquid m^3/h				0.4394
Std vapour 0°C m^3/h				546.6268
C_p kJ/kg-K				4.1851

Z factor				0.0009
Viscosity N-s/m^2				0.0009227
Thermal cond W/mK				0.6062
Surface tension N/m				0.0721
		Component Flow rates in kg/h		
Methane	297.6744	297.6744	297.6744	0.0000
Carbon Dioxide	161.1540	161.1540	161.1540	0.0001
Hydrogen Sulphide	1.6115	1.6115	1.6115	0.0001
Water	0.0000	0.0000	0.0000	439.3520

Stream No.	5	6	7	8
Name	Feed Water	Biogas	Pinch Stream	Flash Water
		Overall		
Molar flow kmol/h	2976.9014	17.9200	2981.2454	2981.2568
Mass flow kg/h	53630.6445	287.6374	53803.4453	53803.4453
Temperature °C	25.2700	25.2561	25.3952	26.4489
Pressure bar	10.0000	10.0000	10.0038	10.0038
Vapour mole fraction	0.0000	1.000	0.0000	4.413E-006
Enthalpy MJ/h	-8.5041×10^{5}	-1361.3	-8.5189×10^{5}	-8.5166×10^{5}
T_c °C	374.1854	-81.5308	373.3960	373.3979
P_c bar	221.1650	45.8068	220.2804	220.2827
Std. sp gr. wtr = 1	1.000	0.301	0.999	0.999
Std. sp gr. air = 1	0.622	0.554	0.623	0.623
Degree API	10.0024	338.8743	10.1607	10.1604
Average mol weight	18.0156	16.0512	18.0473	18.0472
Actual density kg/m^3	996.6185	6.6152	994.2790	993.3415
Actual volume m^3/h	53.8126	43.4815	54.1130	54.1641
Std liquid m^3/h	53.6316	0.9562	53.8646	53.8645
Std vapour 0°C m^3/h	66723.2188	401.6520	66820.5781	66820.8438
		Vapour only		
Molar flow kmol/h		17.9200		0.0132
Mass flow kg/h		287.6374		0.2130
Average mol weight		16.0512		16.1881
Actual density kg/m^3		6.6152		6.6463
Actual volume m^3/h		43.4815		0.0320
Std liquid m^3/h		0.9562		0.0007
Std vapour 0°C m^3/h		401.6520		0.2948
C_p kJ/kg-K		2.2231		2.2075
Z factor		0.9781		0.9783
Viscosity N-s/m^2		1.129×10^{-5}		1.136×10^{-5}
Thermal cond W/mK		0.0345		0.0346
		Liquid only		
Molar flow kmol/h	2976.9014		2981.2454	2981.2439
Mass flow kg/h	53630.6445		53803.4453	53803.2344
Average mol weight	18.0156		18.0473	18.0472
Actual density kg/m^3	996.6185		994.2790	993.9256
Actual volume m^3/h	53.8126		54.1130	54.1321
Std liquid m^3/h	53.6316		53.8646	53.8638

Std vapour 0°C m^3/h	66723.2188		66820.5781	66820.5469
C_p kJ/kg-K	4.1851		4.1874	4.1861
Z factor	0.0085		0.0085	0.0085
Viscosity N-s/m^2	0.0009186		0.0009122	0.0008915
Thermal cond W/mK	0.6065		0.6015	0.6028
Surface tension N/m	0.0720		0.0708	0.0706
		Component Flow rates in kg/h		
Methane	0.0167	286.5063	11.1849	11.1850
Carbon Dioxide	0.9208	0.0217	162.0531	162.0543
Hydrogen Sulphide	2.5891	0.0285	4.1722	3.7365
Water	53627.1133	1.0809	53626.0000	53626.4727

Stream No.	9	10	11	12
Name	Waste Product		Feed Biogas	Recover Water
		Overall		
Molar flow kmol/h	28.7439	2952.5132	22.2638	2952.5132
Mass flow kg/h	612.1639	53191.2852	460.4400	53191.2852
Temperature °C	95.0000	95.0000	25.0000	25.0000
Pressure bar	1.0000	1.0000	10.0000	1.0000
Vapour mole fraction	1.000	0.0000	1.000	0.0000
Enthalpy MJ/h	-7309.5	-8.2791×10^5	-2843.9	-8.4350×10^5
T_c °C	298.0362	374.1853	-64.4918	374.1853
P_c bar	145.8204	221.1647	49.1535	221.1647
Std. sp gr. wtr = 1	0.911	1.000	0.387	1.000
Std. sp gr. air = 1	0.735	0.622	0.714	0.622
Degree API	23.8854	10.0024	233.9444	10.0024
Average mol weight	21.2972	18.0156	20.6811	18.0156
Actual density kg/m^3	0.7011	961.3207	8.5621	996.6862
Actual volume m^3/h	873.1456	55.3315	53.7767	53.3681
Std liquid m^3/h	0.6722	53.1923	1.1892	53.1923
Std vapour 0°C m^3/h	644.2546	66176.5859	499.0139	66176.5859
		Vapour only		
Molar flow kmol/h	28.7439		22.2638	
Mass flow kg/h	612.1639		460.4400	
Average mol weight	21.2972		20.6811	
Actual density kg/m^3	0.7011		8.5621	
Actual volume m^3/h	873.1456		53.7767	
Std liquid m^3/h	0.6722		1.1892	
Std vapour 0°C m^3/h	644.2546		499.0139	
C_p kJ/kg-K	1.6404		1.7377	
Z factor	0.9925		0.9745	
Viscosity N-s/m^2	1.318×10^{-5}		1.242×10^{-5}	
Thermal cond W/mK	0.0245		0.0311	
		Liquid only		
Molar flow kmol/h		2952.5132		2952.5132
Mass flow kg/h		53191.2852		53191.2852
Average mol weight		18.0156		18.0156
Actual density kg/m^3		961.3207		996.6863

Actual volume m^3/h		55.3315		53.3681
Std liquid m^3/h		53.1923		53.1923
Std vapour 0°C m^3/h		66176.5859		66176.5859
C_p kJ/kg-K		4.2127		4.1851
Z factor		0.0007		0.0009
Viscosity N-s/m^2		0.0002969		0.0009227
Thermal cond W/mK		0.6733		0.6061
Surface tension N/m		0.0595		0.0721
Component Flow rates in kg/h				
Methane	11.1683	0.0167	297.6744	0.0167
Carbon Dioxide	161.1335	0.9208	161.1540	0.9208
Hydrogen Sulphide	1.1475	2.5890	1.6115	2.5890
Water	438.7146	53187.7578	0.0000	53187.7578

Stream No.	13
Name	
Overall	
Molar flow kmol/h	2976.9014
Mass flow kg/h	53630.6367
Temperature °C	25.0000
Pressure bar	1.0000
Vapour mole fraction	0.0000
Enthalpy MJ/h	-8.5047×10^5
T_c °C	374.1854
P_c bar	221.1650
Std. sp gr. wtr = 1	1.000
Std. sp gr. air = 1	0.622
Degree API	10.0024
Average mol weight	18.0156
Actual density kg/m^3	996.6865
Actual volume m^3/h	53.8089
Std liquid m^3/h	53.6316
Std vapour 0°C m3/h	66723.2109
Liquid only	
Molar flow kmol/h	2976.9014
Mass flow kg/h	53630.6367
Average mol weight	18.0156
Actual density kg/m^3	996.6865
Actual volume m^3/h	53.8089
Std liquid m^3/h	53.6316
Std vapour 0°C m3/h	66723.2109
C_p kJ/kg-K	4.1851
Z factor	0.0009
Viscosity N-s/m^2	0.0009227
Thermal cond W/mK	0.6061
Surface tension N/m	0.0721
Component Flow rates in kg/h	
Methane	0.0167

Carbon Dioxide	0.9208
Hydrogen Sulphide	2.5891
Water	53627.1094

TABLE 7. Simulated process mass and energy balance

Overall Mass Balance				
	kmol/h		kg/h	
	Input	Output	Input	Output
Methane	18.555	18.555	297.674	297.675
Carbon Dioxide	3.662	3.662	161.154	161.155
Hydrogen Sulphide	0.047	0.035	1.612	1.176
Water	24.388	24.413	439.352	439.795
Total	46.652	46.664	899.792	899.801

Overall Energy Balance [MJ/h]		
	Input	Output
Feed Streams	-9796.1	
Product Streams		-8670.79
Total Heating	16437.5	
Total Cooling	-15592.6	
Power Added	286.499	
Power Generated	0	
Total	-8664.69	-8670.79

CHEMCAD 7.1.2

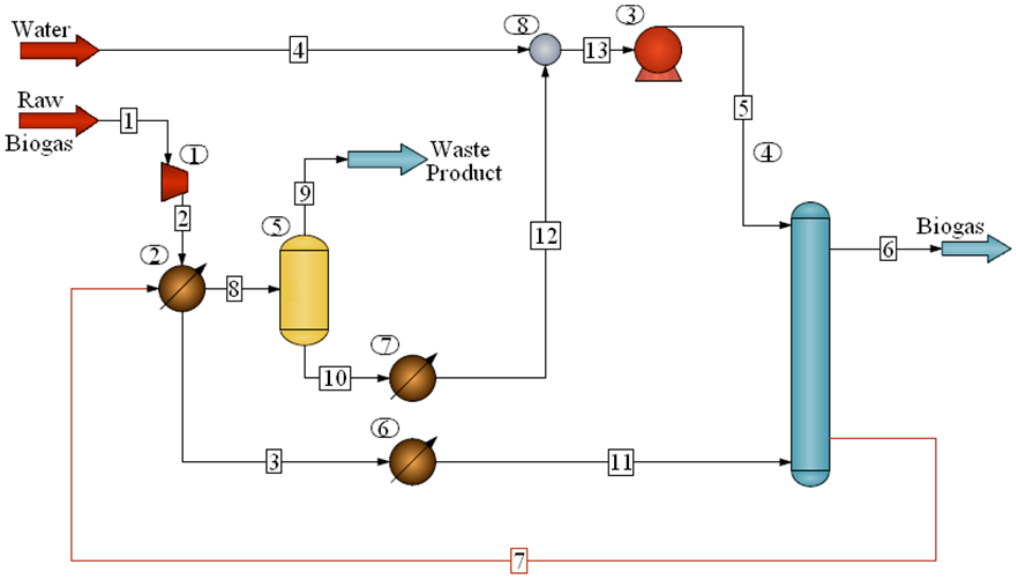

Raw biogas is compressed to 10 bars then cooled down in heat exchanger 2 and 6. Compressed raw biogas (11) is washed counter current in the water scrubber column 4 at 25ºC. Wash water is recovered in flashing drum 5 for recycling (12).

FIGURE 8. Simulated POME biogas purification process flow diagram

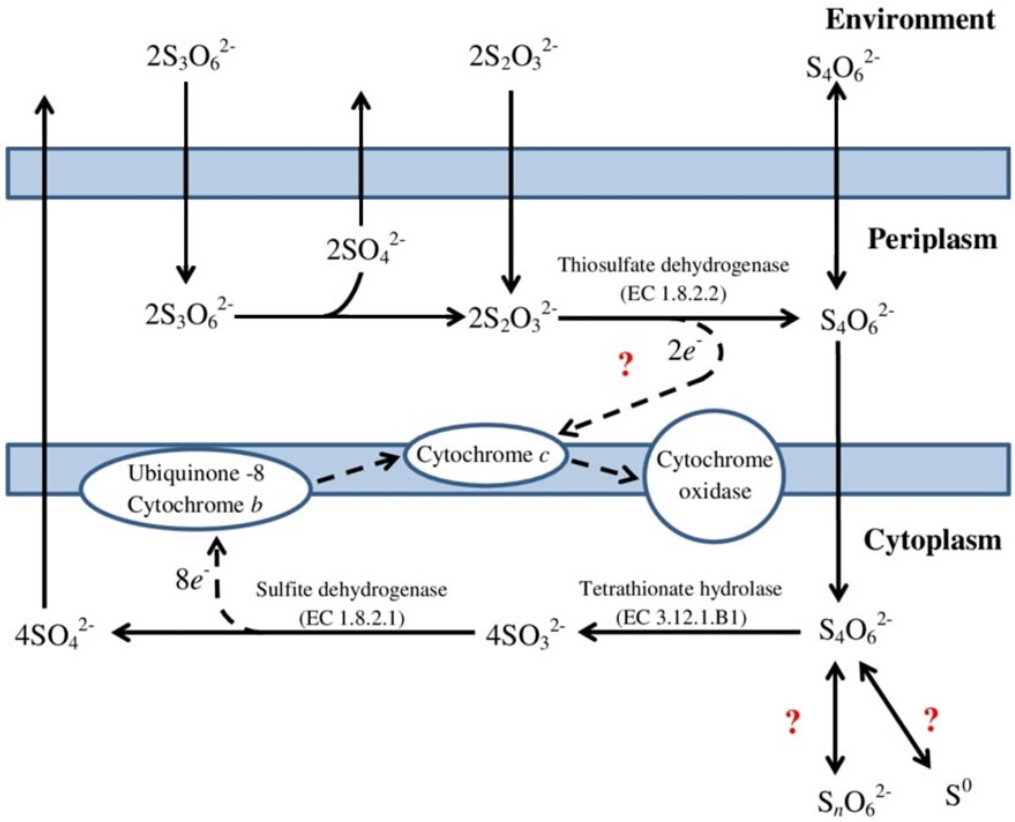

FIGURE 9. Kelly-Trudinger pathway for reduced inorganic sulphur compounds oxidation

Biological scrubbers may be an alternative to avoid high liquid-gas ratio process for biogas purification using chemotropic *Thiobacillus*. All *Thiobacillus* species are obligate autotrophs utilizing elementary sulphur, thiosulfate or polythionates via the Kelly-Trudinger pathway as energy sources and assimilate carbon dioxide for nutrients synthesis (Aminullah et al. 2017). H_2S and CO_2 contents in raw biogas could be reduced with low operating costs. However, Figure 9 shows that the Kelly-Trudinger pathway has yet to be fully understood.

Chemical scrubber also shows the potential for the biogas purification task mainly via reaction as follows:

$$2NaOH + CO_2 \rightarrow Na_2CO_3 + H_2O$$

but the operational cost may be higher due to chemical consumption and solvent recovery.

CONCLUSION

Water scrubber system is well understood and economically viable for many chemical purification processes. The ChemCAD simulation shows that water scrubber POME biogas purification process is feasible to produce high purity of methane suitable to be used as a sustainable IC engine fuel at 10 bar pressure and 25°C ambient temperature. Further simulations may be carried out using different washing medium for CAPEX and OPEX comparisons.

ACKNOWLEDGEMENTS

The authors would like to thank Director General of Malaysian Palm Oil Board for his kind permission to publish this paper.

DECLARATION OF COMPETING INTEREST

None.

REFERENCES

Ahmad Parveez, G K., Astimar, A. A. & Rohaya, M. H. 2020. *Palm Oil Milling and Processing Handbook*. Bangi: Malaysian Palm Oil Board

Aminullah, M., Ho, W. S., Hashim, H., Lim, J. S., Abdul Muis, Z. & Liew, P. Y. 2017. Palm oil mill effluent (POME) biogas off-site utilization Malaysia specification and legislation. *Chemical Engineering Transactions* 56: 637–642.

Branan, C. 2002. *Rules of Thumb for Chemical Engineers*. 3rd edition. Amsterdam: Gulf Professional Publishing.

Carroll, J. J., Slupsky, J. D. & Mather, A. E. 1991. *The* solubility of carbon dioxide in water at low pressure. *Journal of Physic Chemistry Reference Data* 20(6): 1201–1209.

Coulson. J. M., Richardson, J. F. & Sinnott, R. K. 1989. *Chemical Engineering Volume 6: An Introduction to Chemical Engineering Design.* Oxford: Pergamon Press Ltd.

Dean, J. A. 1999. *Lange's Handbook of Chemistry.* 10th edition. USA: McGraw-Hill, Inc. p. 1100

Duan, Z. & Sun, R. 2003. An improved model calculating CO2 solubility in pure water and aqueous NaCl solutions from 273 to 533 K and from 0 to 2000 bar. *Chemical Geology* 193(3-4): 257-271.

EPA. 2011. *2011 US Greenhouse Gas Inventory Report*. USEPA #430-R-11-005: United States Environmental Protection Agency.

Fueller, E. N., Schettler, P. D. and Giddings, J. C. 1966. New method for prediction of binary gas-phase diffusion coefficients. *Ind. Eng. Chem*., 58(5): 18-27.

Gautam T K. 2014. The outlook for fuels for internal combustion engines. *International Journal of Engine Research* 15(4): 383–398.

Jaole, D. G., Ghugare, G. S. & Murthy, T. S. N. 1995. Pressure drop behaviour for high liquid-gas ratios in packed column. *Indian Journal of Engineering & Materials Sciences* 2: 221–223.

Loh, S. K., Nasrin, A. B., Mohamad Azri, S., Nurul Adela, B., Muzzammil, N., Daryl Jay, T., Stasha Eleanor, R. A., Lim, W. S., Choo, Y. M. & Kaltschmitt, M. 2017. First report on Malaysia's experiences and development in biogas capture and utilization from palm oil mill effluent under the Economic Transformation Programme: current and future perspectives. *Renew. Sustain. Energy Rev.* 74: 1257-1274. DOI:10.1016/j.rser.2017.02.066.

MPOB. 2020. *Overview of the Malaysian Oil Palm Industry 2019*. Bangi: Malaysian Palm Oil Board.

Nock, W. J., Walker, M., Kapoor, R. & Heaven, S. 2014. Modeling the water scrubbing process and energy requirements for co_2 capture to upgrade biogas to biomethane. *Ind. Eng. Chem. Res.* 53(32): 12783-12792.

Perry, R. H., Green, D. W. & Maloney, J. O. 1997. Physical and Chemical Data Table 2-125. *Perry's Chemical Engineers' Handbook*. Seventh Edition. United States of America: The McGraw-Hill Companies, Inc.

Ralph, F. & Strigle, Jr. 1994. *Packed Tower Design and Application: Random and Structured Packings.* 2nd edition. Houston: Gulf Publishing Company.

Spycher, N., Pruess, K. & Ennis-King, J. 2003. CO2-H2O mixture in the geological sequestration of CO2. I. Assessment and calculation of mutual solubilities from 12 to 100oC and up to 600 bar. *Geochimica et Cosmochimica Acta* 67(16): 3015-3031.

Stefan, M. 2004. *Biogas* fuel for internal combustion engines. A*nnals of the Faculty of Engineering Hunedoara*. TOME II. *Fascicole* 3: 179–190.

Thome, J. R. 2004. *Engineering Data Book III*. USA: Wolverine Tube Inc.

Wilke, C.R. & Chang, P. 1955. Correlation of diffusion coefficients in dilute solutions. AIChE, 1(2).

Winterbone, D. & Turan, A. 2015. Thermodynamic properties of ideal gases and ideal gas mixtures of constant composition. *Advanced Thermodynamics for Engineers*, 177-205.

NOMENCLATURE

Symbol	Particular	SI Unit
A	Column cross sectional area	m^2
A_c	Column area	m^2
A_G	Vapor phase channel cross-section area	m^2
A_L	Liquid phase channel cross-section area	m^2
A_w	Effective interfacial packing area	m^2m^{-3}
C	Molar concentration of CO_2 in biogas	mol m^{-3}
C_s	Fixed temperature gas equilibrium solubility	-
D	Column diameter	m
D_L	Liquid diffusity	m^2s^{-1}
D_v	Gas diffusivity	m^2s^{-1}
F_B	Biogas molar flow rate	mol s^{-1}
F_L	Water molar flow rate	mol s^{-1}
F_p	Packing factor	-
H	Packed bed height	m
H_G	Gas film transfer unit height	m
H_L	Liquid film transfer unit height	m
H_{LG}	Overall transfer unit height	m
K_G	Overall gas-phase mass transfer coefficient	ms^{-1}
L_G	Beam line length through vapor phase	m
L_L	Beam line length through liquid phase	m
N_T	Transfer unit number	-
P_G	Partial pressure for ideal gas *G*	Nm^{-2}
P_T	Total pressure	Nm^{-2}
P_{C1}	Partial pressure of CO_2 at inlet biogas	Nm^{-2}
P_{C2}	Partial pressure of CO_2 at outlet biogas	Nm^{-2}
R	Universal gas constant	$J(kg.K)^{-1}$
T	Temperature	°C
U	Superficial fluid velocity	ms^{-1}
V_G	Vapor phase channel volume	m^3
V_L	Liquid phase channel volume	m^3
V_p	Tower packing volume	m^3
W_G	Molecular weight for gas *G*	-
$f(r,t)$	Local instantaneous at radius *r* and time *t*	-
g	Gravitational acceleration	ms^{-2}
k	Henry's law constant	Pa
k_e	Equilibrium constant	-
k_G	Gas film mass transfer coefficient	$kg/(m^2s.Pa)$
k_L	Liquid film mass transfer coefficient	$kgm^{-2}s^{-1}$
m	Slope of equilibrium line	-
r	Radius	m
s_i	Molar solubility for gas *i*	mol m^{-3}
t	Time	s

x_e	Packing equivalent spherical diameter	m
x	Mole fraction in water phase	-
y	Mole fraction in gas phase	-
$-\Delta P$	Pressure drop	Pa
α	Interfacial are per unit volume	$m^2\,m^{-3}$
ρ	Density	kgm^{-3}
σ	Surface tension	Nm^{-1}
μ	Dynamic viscosity	Nsm^{-2}
ε	Packing void fraction	
γ	Activity coefficient in water	
φ	Fugacity coefficient	
λ	Molar density	$mol\,m^{-3}$

APPENDIX

CARBON DIOXIDE SOLUBILITY IN WATER AT VARIOUS TEMPERATURES AND PRESSURES

Table A1 shows the solubility of CO_2 in water, expressed as CO_2 mole fraction in the liquid phase, is given for partial pressures up to 100kPa and temperatures of 0°C to 100°C. Note that one (1) standard atmosphere equals 101.325kPa. The references give data over a wider range of temperature and partial pressure. The estimated uncertainty is about 2%.

Gas i molar solubility, s_i is given as $k_e \frac{\varphi_i P_i}{\gamma_i}$, where γ is the activity coefficient in water, k_e is the equilibrium constant, P is the partial pressure, and φ is the fugacity coefficient. Based on critical pressure and temperature, fugacity coefficient is determined using Peng-Robinson state equation (Peng and Robinson, 1976). Gas acentric factor in a gas mixture determines the limiting volume and the Van der Waals equation defines the attraction factor. The fugacity coefficient is close to 1 when the total pressure of the gas phase is less than about 10 atm, thus can be neglected in the solubility calculation. However, Figure A1 shows substantial effect at higher pressures for CO_2. At low pressures, CO_2 concentration increases near-linearly with pressure. At 25 °C and pressures higher than 62 atm, the concentration increases more gradually as the fugacity coefficient drops rapidly.

GASES DIFFUSIVITIES

Gases diffusivity coefficient, D_v could be predicted using Fuller et al. (1966) equation with data presented in Table A5.

$$D_v = \frac{1.013\times10^{-7}T^{1.75}\left(\frac{1}{W_a}+\frac{1}{W_b}\right)^{0.5}}{P_T[(\sum v_i)_a^{1/3}+(\sum v_i)_b^{1/3}]^2} \quad \text{(A1)}$$

where T = Temperature [K]; W_a, W_b = Molecular weights for components a and b; P = Total pressure [bar] and $\sum v_i$ = Summation of the special atomic diffusion volume coefficients for respective components given in *Table A5*.

LIQUID DIFFUSIVITIES

Liquid diffusivity coefficient, D_L could be predicted using Wilke & Chang (1955) equation with data presented in Table A6.

$$D_L = \frac{1.173\times10^{-13}(\varphi W)^{0.5}T}{\mu V^{0.6}} \quad \text{(A2)}$$

where W = Solvent molecular weight, μ = Solvent viscosity [$mNsm^{-2}$], V = Solvent molar volume at boiling point [$m^3(kmol)^{-1}$] calculated from data shown in Table A6, ϕ= Association factor for the solvent; ϕ= 2.6 for water; ϕ= 1.9 for methanol; ϕ= 1.5 for ethanol and ϕ= 1.0 for unassociated solvents.

TABLE A1. CO_2 solubility in H_2O at various temperatures and partial pressures (Source: Fernandez-Prini & Crovetto, 1989; Carroll et al. 1991; Crovetto, 1991)

T [°C]	Partial pressure of CO_2 [kPa]						
	5	10	20	30	40	50	100
0	0 .067	0 .135	0 .269	0 .404	0 .538	0 .671	1 .337
5	0 .056	0 .113	0 .226	0 .338	0 .451	0 .564	1 .123
10	0 .048	0 .096	0 .191	0 .287	0 .382	0 .477	0 .950
15	0 .041	0 .082	0 .164	0 .245	0 .327	0 .409	0 .814
20	0 .035	0 .071	0 .141	0 .212	0 .283	0 .353	0 .704
25	0 .031	0 .062	0 .123	0 .185	0 .247	0 .308	0 .614
30	0 .027	0 .054	0 .109	0 .163	0 .218	0 .271	0 .541
35	0 .024	0 .048	0 .097	0 .145	0 .193	0 .242	0 .481
40	0 .022	0 .043	0 .087	0 .130	0 .173	0 .216	0 .431
45	0 .020	0 .039	0 .078	0 .117	0 .156	0 .196	0 .389
50	0 .018	0 .036	0 .071	0 .107	0 .142	0 .178	0 .354

55	0 .016	0 .033	0 .065	0 .098	0 .131	0 .163	0 .325
60	0 .015	0 .030	0 .060	0 .090	0 .121	0 .150	0 .300
65	0 .014	0 .028	0 .056	0 .084	0 .112	0 .140	0 .279
70	0 .013	0 .026	0 .052	0 .079	0 .105	0 .131	0 .261
75	0 .012	0 .025	0 .049	0 .074	0 .099	0 .123	0 .245
80	0 .012	0 .023	0 .047	0 .070	0 .093	0 .116	0 .232
85	0 .011	0 .022	0 .044	0 .067	0 .089	0 .111	0 .221
90	0 .011	0 .021	0 .042	0 .064	0 .085	0 .106	0 .211
95	0 .010	0 .020	0 .041	0 .061	0 .082	0 .102	0 .203
100	0 .010	0 .020	0 .039	0 .059	0 .079	0 .098	0 .196

Note: 1000 × mole fraction of CO_2 in liquid phase

TABLE A2. CO_2 aqueous solubility at 101.3 kPa (1 atm) (Source: Dean, 1999)

T [°C]	Dissolved CO_2		***T*** [°C]	Dissolved CO_2	
	v/v H_2O	g/100ml H_2O		v/v H_2O	g/100ml H_2O
0	1.713	0.3346	18	0.928	0.1789
1	1.646	0.3213	19	0.902	0.1737
2	1.584	0.3091	20	0.878	0.1688
3	1.527	0.2978	21	0.854	0.1640
4	1.473	0.2871	22	0.829	0.1590
5	1.424	0.2774	23	0.804	0.1540
6	1.377	0.2681	24	0.781	0.1493
7	1.331	0.2589	25	0.759	0.1449
8	1.282	0.2492	26	0.738	0.1406
9	1.237	0.2403	27	0.718	0.1366
10	1.194	0.2318	28	0.699	0.1327
11	1.154	0.2239	29	0.682	0.1292
12	1.117	0.2165	30	0.655	0.1257
13	1.083	0.2098	35	0.592	0.1105
14	1.050	0.2032	40	0.530	0.0973
15	1.019	0.1970	45	0.479	0.0860
16	0.985	0.1903	50	0.436	0.0761
17	0.956	0.1845	60	0.359	0.0576

Notes: The solubility is given for "pure water", i.e. water which contains only CO_2. This water is acidic. For example, at 25 °C, pH 3.9 is expected. At less acidic pH values, the solubility will increase due to the pH-dependent speciation of CO_2.

TABLE A3. Aqueous solubility in weight of CO_2 per 100 weight of H_2O at various pressures (Source: Perry et al. 1997)

P [atm]	*T* [°C]								
	12	18	25	31.04	35	40	50	75	100
25		3.86	3.29	2.80	2.56	2.30	1.92	1.35	1.06
50	7.03	6.33	5.38	4.77	4.39	4.02	3.41	2.49	2.01
75	7.18	6.69	6.17	5.80	5.51	5.10	4.45	3.37	2.82
100	7.27	6.72	6.28	5.97	5.76	5.50	5.07	4.07	3.49
150				6.25	6.03	5.81	5.47	4.86	4.49
200				6.48	6.29	6.28	5.76	5.27	5.08
300	7.86	7.35					6.20	5.83	5.84
400	8.12	7.77	7.54	7.27	7.06	6.89	6.58	6.30	6.40
500				7.65	7.51	7.26			
700							7.58	7.43	7.61

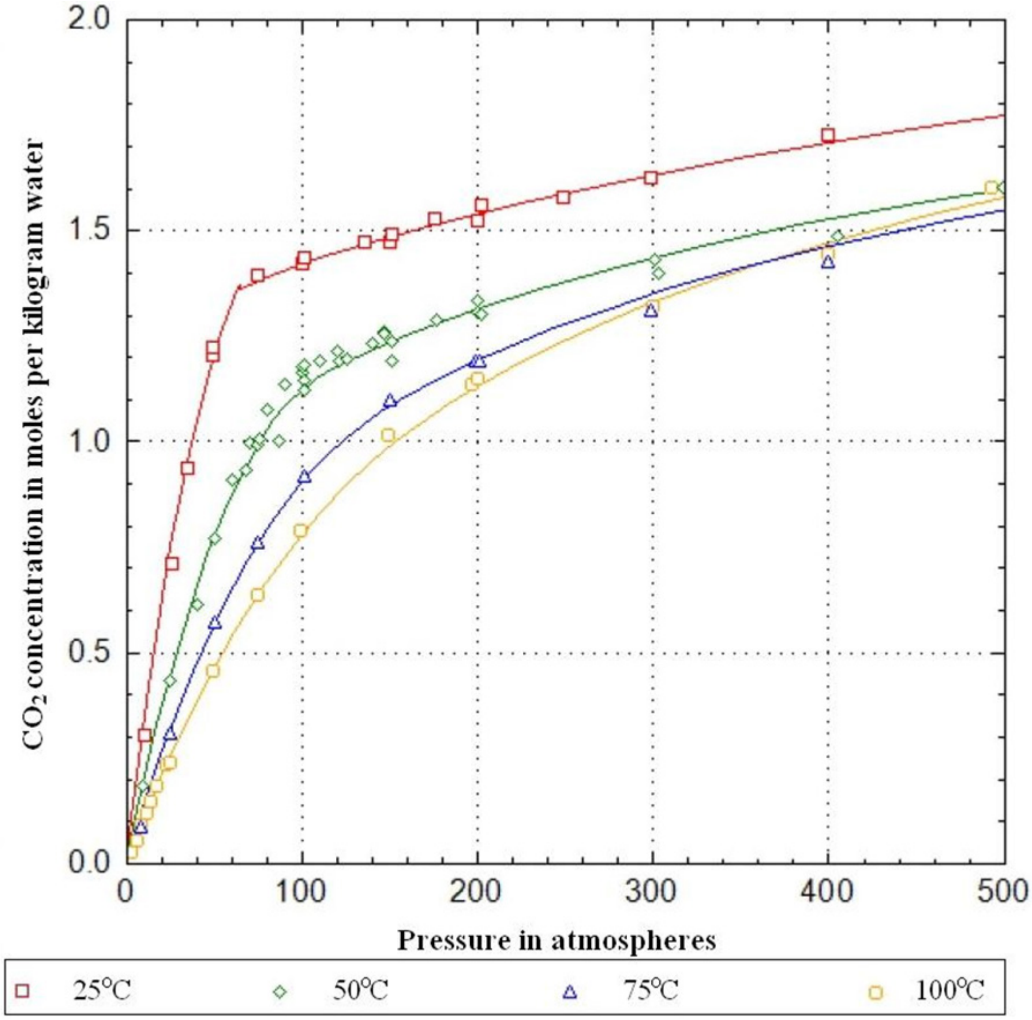

FIGURE A1. CO_2 solubility as a function of gas pressure at 25°C, 50°C, 75 and 100°C. Data points are from compilations by Duan *et al*. (2003) and Spycher *et al.* (2003).

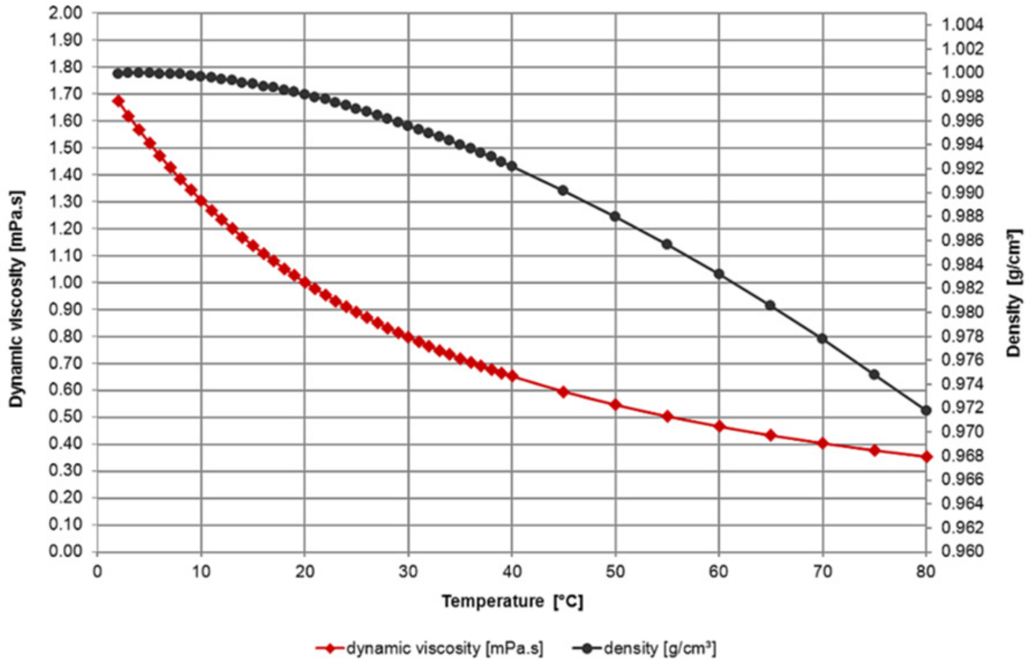

FIGURE A2. Water dynamic viscosity and density for various temperatures

TABLE A4. Various metal packing materials characteristic

Pall Rings	Size	Nos. / m^3	α [m^2/m^3]	ε [%]	F_p
	13 mm	4,00,000	430	90	73
	16 mm	2,10,000	345	93.1	71
	19 mm	1,00,000	250	94	63
	25 mm	51,000	208	94.5	48
	38 mm	13,500	131	95	28
	50 mm	6,500	98	96	20
	75 mm	1,820	71	96	18
IMTP / Saddles					
	No. 15	3,47,500	290	95	51
	No. 25	1,36,500	226	96.2	41
	No. 40	50,000	150	97.3	24
	No. 50	14,750	99	98	18
	No. 70	4,625	59	98	12
Raschig Rings	[mm]				
	8 x 8	1500000	630	91	
	10 x 10	770000	500	89	
	12 x 12	450000	430	90	300
	15 x 15	230000	350	92	260
	25 x 25	51000	220	92	137
	35 x 35	19000	150	93	
	38 x 38	14000	130	93	83
	50 x 50	6500	110	95	57
	80 x 80	1600	65	96	32
	100 x 100	750	48	96	

TABLE A5. Special atomic diffusion volumes (Fueller et al. 1966)

C	H	O	N	Cl	S	rings
16.5	1.98	5.48	5.69	19.5	17.0	-20.0
Simple Molecules Diffusion Volume						
H_2	D_2	He	N_2	O_2	air	Ne
12.7	6.70	2.88	17.9	16.6	20.1	5.59
Ar	Kr	Xe	CO	CO_2	N_2O	NH_3
16.1	22.8	37.9	18.9	26.9	35.9	14.9
CCL_2	F_2	SF_6	Cl_2	Br_2	SO_2	
114.8	114.8	69.7	37.7	67.2	41.1	

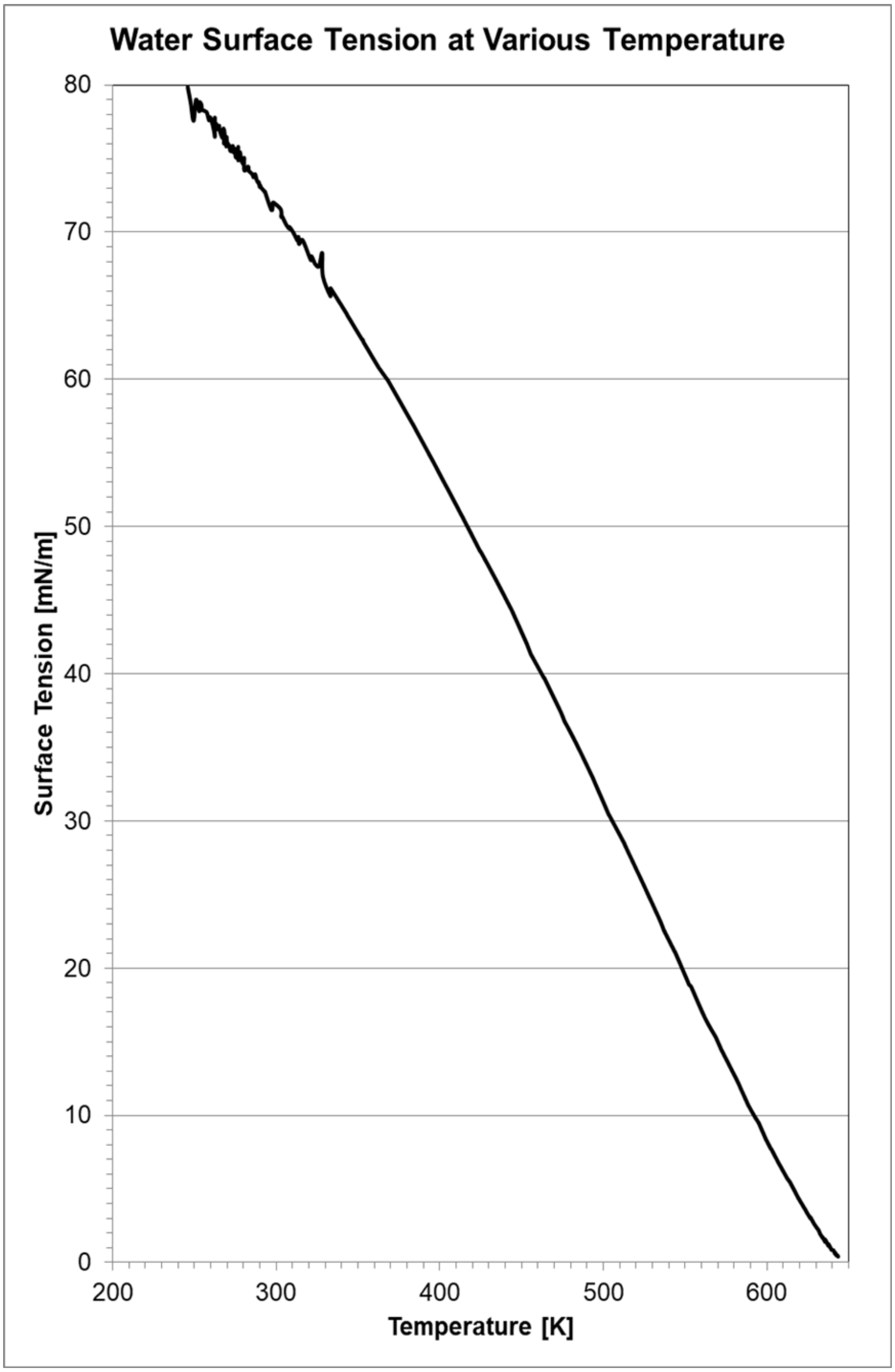

FIGURE A3. Water surface tension at various temperatures

TABLE A6. Structural contribution to molar volumes (Source: Wilke & Chang, 1955)

Molecular Volumes							
Air	0.0299	CO_2	0.0340	H_2S	0.0329	NO	0.0236
Br_2	0.0532	COS	0.0515	I_2	0.0715	N_2O	0.0364
Cl_2	0.0484	H_2	0.0143	N_2	0.0312	O_2	0.0256
CO	0.0307	H_2O	0.0189	NH_3	0.0258	SO_2	0.0448
Atomic Volumes							
As	0.0305	F	0.0087	P	0.0270	Sn	0.0423
Bi	0.0480	Ge	0.0345	Pb	0.0480	Ti	0.0357
Br	0.0270	H	0.0037	S	0.0256	V	0.0320
C	0.0148	Hg	0.0190	Sb	0.0342	Zn	0.0204
Cr	0.0274	I	0.0370	Si	0.0320		

Complex Organic Volumes			
Cl terminal as in RCl	0.0216	Oxygen, except as noted below	0.0074
• medial as in R-CHCl-R	0.0246	• in methyl esters	0.0091
Nitrogen double-bonded	0.0156	• in methyl ethers	0.0099
• triply bonded as in nitrile	0.0162	• in higher esters, ethers	0.0110
• primary amines, RNH_2	0.0105	• in acids	0.0120
• secondary amines, R_2NH	0.0120	• in union with S, P, N	0.0083
• tertiary amines, R_3N	0.0108	• three-member ring	-0.0060
Naphthalene ring	-0.0300	• four-member ring	-0.0085
Anthracene ring	-0.0475	• five-member ring	-0.0115
		• six-member ring	-0.0150
		(benzene, cyclohexane, pyridine)	